TECHNICAL REVIEW

Dual-layer Microphone Array
Acoustic Intensity Probe Calibrator
Multi-field Microphone

Brüel & Kjær

creating sustainable value

Previously issued numbers of Brüel & Kjær Technical Review

Technical Review

No. 1 – 2011

Contents

TRADEMARKS

PULSE is a trademark of Brüel & Kjær Sound & Vibration Measurement A/S

Editor: Harry K. Zaveri

Performance Investigation of the Dual-Layer Array (DLA) at Low Frequencies

Jørgen Hald

Abstract

A dual-layer array with 3 cm separation between layers and with 3 cm microphone pitch in each layer is designed to cover frequencies up to approximately 5000 Hz. The performance is best in the frequency range from a few hundred Hertz up to 5 kHz. At lower frequencies phase mismatch between the microphones becomes very critical. However, in many applications it is desirable to be able to measure down to, for example, 100 Hz, even in very reactive sound fields such as a car cabin or an aircraft cabin.

This article investigates the capability of an array containing two parallel layers with 8×8 microphones in each layer and with 3 cm microphone pitch to measure sound intensity at low frequencies in sound fields with strong reactive or diffuse components. This is done basically by extending the concept of pressure-residual-intensity (p-RI) index from two-microphone intensity probe measurements to array measurements and by estimation of that index based on both simulated and real measurements. Good agreement is achieved between p-RI indices obtained from simulated measurements and from real measurements in a large standing wave tube. It is shown that for typical array microphones it is essential to correct for the differing frequency responses, typically based on response data stored in the Transducer Electronic Data Sheets (TEDS) of the individual microphones.

To investigate whether the changes in static pressure during flight will cause too large spreading of the phase responses, a series of measurements was taken in a depressurized chamber used for flight simulations. The main conclusion was that above approximately 200 Hz, measurements can be taken without performing in-flight phase calibration.

Résumé

Une antenne microphonique double couche avec 3 cm de séparation entre couches et un espacement de microphone de 3 cm sur chaque couche est conçue pour couvrir les fréquences jusqu'à environ 5000 Hz. Les meilleures performances sont atteintes entre quelques centaines de Hertz et 5 kHz. Aux fréquences plus basses, la différence de phase entre les microphones devient critique. Toutefois, dans de nombreuses applications, il est souhaitable de pouvoir mesurer jusqu'à des fréquences aussi basses que 100 Hz, même lorsque les champs acoustiques sont très réactifs, notamment dans les habitacles de véhicules ou les cabines d'avions.

Le présent article étudie la performance d'une antenne de 8×8 microphones espacés de 3 cm sur chacune des deux couches parallèles, et sa capacité à mesurer aux basses fréquences l'intensité acoustique de champs sonores dont les composantes sont diffuses et très réactives. Ces investigations s'effectuent en étendant aux mesurages par antennerie acoustique la méthode basée sur l'indice pression-intensité résiduelle (p-RI) entre les deux microphones d'une sonde d'intensimétrie. L'estimation de cet indice se base sur des mesurage simulées et les mesurages réels. Un bonne correspondance est obtenue entre les indices résultant de mesures simulées et ceux résultant de mesures réelles obtenues au moyen d'un tube à onde stationnaire. Il est montré que, pour une antenne microphonique typique, il est indispensable de corriger la différence entre réponses en fréquence, généralement en s'aidant des données mémorisées dans les fiches électroniques Transducer Electronic Data Sheets (TEDS) des microphones.

Pour étudier si les changements de pression statique au cours d'un vol entraînent une dispersion trop importante des réponses en phase, une série de mesurages a été effectuée dans une chambre d'essai dépressurisée servant de simulateur de vol. Elle a mené à la conclusion que, au-dessus de 200 Hz environ, les mesures peuvent être obtenues sans qu'il soit nécessaire de procéder à un calibrage de phase en vol.

Zusammenfassung

Ein doppelseitiges Array mit 3 cm Abstand zwischen den beiden Teilarrays und 3 cm Mikrofonabstand soll Frequenzen bis ca. 5000 Hz abdecken. Die beste Leistung wird im Frequenzbereich von wenigen hundert Hertz bis zu 5 kHz erreicht. Bei tieferen Frequenzen wird die Phasenfehlanpassung zwischen den

Mikrofonen sehr kritisch. Bei vielen Anwendungen ist es jedoch wünschenswert, bis hinab zu beispielsweise 100 Hz messen zu können, auch in stark reaktiven Schallfeldern wie in Fahrzeug- oder Flugzeugkabinen.

Im vorliegenden Artikel wird untersucht, wie gut ein Array mit jeweils 8×8 Mikrofonen in zwei parallelen Teilarrays und 3 cm Mikrofonabstand die Schallintensität bei tiefen Frequenzen in Schallfeldern mit starken reaktiven oder diffusen Komponenten messen kann. Zu diesem Zweck wurde das Konzept des p-RI (Pressure-Residual Intensity) index von der Intensitätssondenmessung mit zwei Mikrofonen auf Array-Messungen erweitert und dieser Index auf der Basis von simulierten und wirklichen Messungen abgeschätzt. Es wurde eine gute Übereinstimmung zwischen p-RI indizes erhalten, die anhand von simulierten Messungen und durch wirkliche Messungen in einem großen Impedanzrohr mit stehenden Wellen ermittelt wurden. Es wird gezeigt, dass es bei typischen Arraymikrofonen wichtig ist, Frequenzgangunterschiede zu korrigieren, in der Regel anhand von Frequenzgangdaten, die in den TEDS (Transducer Electronic Data Sheets) der einzelnen Mikrofone gespeichert sind.

Um zu untersuchen, ob die Änderungen des statischen Drucks während des Fluges eine zu große Streuung der Phasenfrequenzgänge verursachen, wurde eine Reihe von Messungen in einer Druckabfallkammer für Flugsimulationen ausgeführt. Daraus konnte abgeleitet werden, dass für Messungen über ca. 200 Hz keine Phasenkalibrierung während des Fluges erforderlich ist.

Nur ein Bruchteil aller akustischen Messungen wird unter den wohldefinierten und kontrollierten Bedingungen eines Kalibrierlaboratoriums ausgeführt – im Gegenteil, die meisten akustischen Messungen erfolgen unter nicht kontrollierten Bedingungen, die in vielen Fällen nicht einmal vorher bekannt sind.

Introduction

Some main characteristics of noise in aircraft and helicopter cabins have been described in reference [1], and reference [2] contains some requirements set by aerospace companies to NSI tools for cabin noise measurements. For business jets the main focus is on the SIL 3 frequency range (1, 2 and 4 kHz octave bands) from 700 Hz up to 5700 Hz, where the main source is Turbulent Boundary Layer (TBL) excitation. The dual-layer array (DLA) has been designed with a main focus on

this SIL frequency range. The upper limiting frequency of 5700 Hz would require an array element spacing not larger than 2.6 cm. With available technology, the distance between the two microphone layers could, however, not be smaller than 3 cm, so the array was constructed with 3 cm element spacing, leading to an upper limiting frequency at 5000 Hz.

The holography calculation algorithm used with the DLA is Statistically Optimized Near-field Acoustic Holography (SONAH) [3–5]. As opposed to standard NAH calculation, SONAH allows the use of a measurement area that is small compared to the total sound source area and which can be also significantly smaller than wavelength. The use of the DLA with the SONAH algorithm for both standard holography calculations and in particular for extraction of Entering Intensity has been described in reference [6].

In the SIL 3 frequency range, the sensitivity of the array processing to realistic microphone mismatch errors is very small. A simulated measurement that illustrates this will be given in **Simulated Measurements**. The main source of error will be diffraction in the mechanical array structure, including the microphones themselves. An investigation of these diffraction errors and their effect on the output from SONAH calculations was described in reference [7]. It was shown that account should be taken for the acoustical centre being a frequency dependent distance in front of the microphones. Such a correction has been implemented in the SONAH processing software.

At frequencies below the SIL 3 range, the influence of phase errors will quickly increase, because the phase variation of the sound field across the array becomes small. With 8×8 elements in each layer, the array size becomes 21×21 cm. For helicopters and propeller aircraft there are strong and sometimes very annoying harmonic noise components at frequencies below 700 Hz, so the array performance at these low frequencies is certainly of interest.

Simulated Measurements investigates the sensitivity of the DLA/SONAH prediction of sound intensity to transducer mismatch errors through:

1) A set of simulated measurements on point sources.
2) The pressure-residual intensity index (p-RI index) resulting from the same pressure applied to all microphones.

Measurement in Standing Wave Tube presents results from an approximate measurement of the p-RI index in a standing wave tube, and finally **Measurements in Under-pressure Chamber** contains results from measurements of the microphone mismatch resulting from a static pressure drop corresponding to the one experienced during flight.

4

Simulated Measurements

To investigate the influence of phase mismatch, a set of simulated measurements on point sources were fist performed. Fig. 1 shows the source configuration. There are 4 monopole point sources shown as red dots – 2 in front of and 2 behind the array – and all point sources are mutually incoherent with equal amplitudes. The chosen source configuration produces a sound field with an average p-I index (ratio) around 5 dB in the region occupied by the array.

Fig. 1. Geometry used in simulated measurements on monopole point sources

(a) Side view *(b) View from back side*
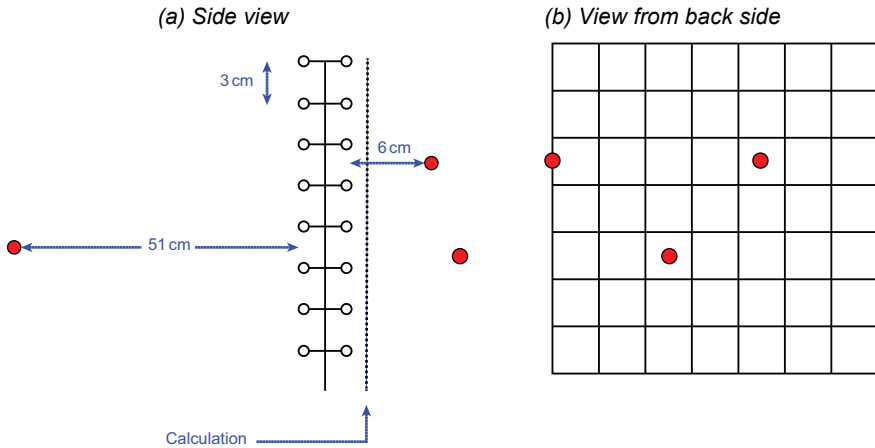
In a real measurement setup we recommend the array to be at a distance from the cabin panel surface around half of the array-grid spacing, i.e., 1 – 2 cm. To approximate that condition, we have here chosen a calculation plane 1.5 cm in front of the array.

A series of 50 measurements were simulated, where independent phase errors were applied to the microphone signals for each new measurement. The phase errors were given a rectangular distribution over an interval centred at 0.0. Based on the noisy measurements, the component of sound intensity normal to the array plane was calculated using SONAH as described in references [4] and [6]. A fixed dynamic range equal to 20 dB and a virtual source plane at $z = -75$ mm was applied in the SONAH processing. The relative average error on the sound intensity was then calculated using the formula:

$$E \equiv 10 \cdot \log\left(\frac{\sum |I - I_0|}{\sum |I_0|}\right) \qquad (1)$$

where I_0 is the true intensity and where the summations are over calculation positions and over the measurements with independent phase error assignments.

Fig. 2 shows the relative average error defined in equation (1) as a function of frequency for two different intervals of the microphone phase error: ±1° and ±0.1°. Over the SIL 3 frequency range (i.e., down to 700 Hz) fairly good intensity estimates can be performed even with phase errors within ±1°, but below 700 Hz, the resulting intensity errors quickly increase. In the range 50 – 200 Hz the phase error should be within approximately ±0.1° to get acceptable intensity estimates

Fig. 2. Relative average Intensity error with ±1° and ±0.1° random phase error
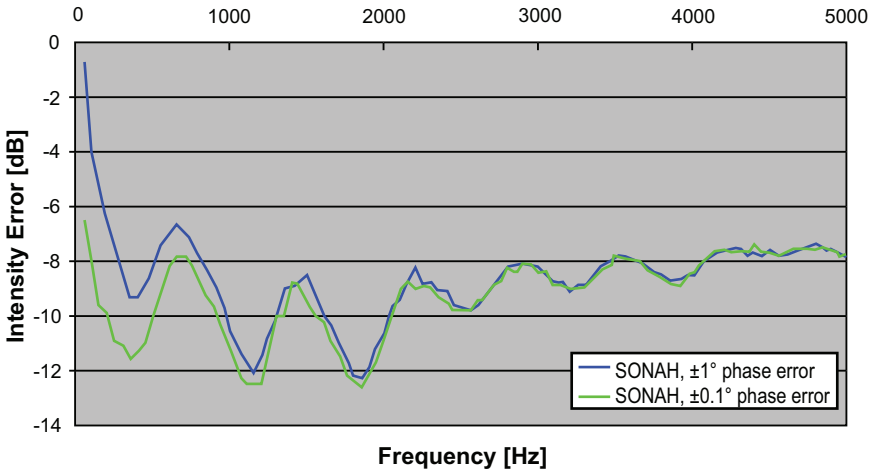
For two-microphone sound intensity probes it is customary to describe the phase-error related dynamic capability in terms of the p-RI index. This quantity is defined as the level difference in decibel between pressure and measured "residual" sound intensity in the case where the same sound pressure is applied to both microphones of the probe, so the intensity should equal zero. A similarly defined p-RI index can be used in connection with measurement of sound intensity using the DLA with SONAH processing. Here, however, the index will depend on

the calculation plane and of the position on that plane. To get a single number for a given calculation plane, one can use averaging over the calculation surface or take a peak value. For the simulated measurements we will use an area averaging.

So to simulate measurements of the p-RI index, we apply the same pressure to all microphones, and just like for the simulated measurements on point sources we add independent phase errors with a rectangular distribution around zero to the individual microphones. The p-RI index is then calculated as:

$$R_{avg} \equiv 10 \cdot \log\left(\frac{|p_0|^2}{|\bar{I}|}\right) \tag{2}$$

where p_0 is the applied constant pressure and $|\bar{I}|$ is the intensity averaged over points on the calculation plane and over 50 simulated measurements with independent phase error assignments. The results of the simulations are shown in Fig. 3. Three sets of simulations are represented:

- Using the calculation plane shown in Fig. 1 (z = −15 mm), and applying phase errors with a rectangular distribution within the interval ±2º. This level of phase error is considered as being representative for microphones without correction for individual frequency responses. This is a worst case scenario
- Using again the calculation plane shown in Fig. 1 (z = −15 mm), but now the interval for the phase errors is reduced to ±0.4º. This level of phase error is considered as being representative for microphones after Frequency Response Correction (FRC) using the responses provided in the Transducer Electronic Data Sheets (TEDS) in the individual microphones
- Using the centre plane (z = +15 mm) between the two microphone layers as calculation plane, and still using TEDS correction. This is the best case

In all cases a 20 dB dynamic range and a virtual source plane at z = −75 mm has been used in the SONAH calculation. The curves give an idea of the dynamic capability of the system with the available phase matching of the microphones. Clearly, the TEDS-based correction provides an important improvement to the dynamic range. These results based on simulated measurements will be compared with results from measurements in the **Measurement in Standing Wave Tube** section.

Fig. 3. p-RI indices from simulated measurements.
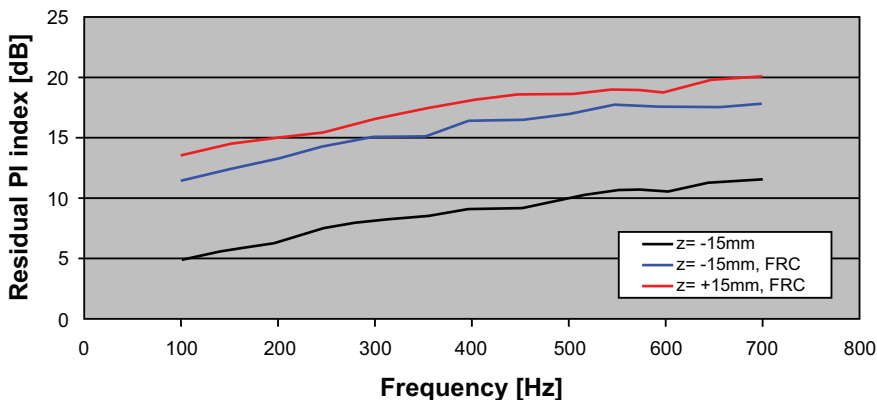
Measurement in Standing Wave Tube

Measuring the p-RI index of the DLA/SONAH system is difficult, because it requires the same pressure to be applied to all microphones. This is almost impossible to achieve with phase errors much lower than ±1º up to 700 Hz. A similar condition could, however, be measured in a large standing wave tube available at Brüel & Kjær SVM A/S, see Fig. 4. The tube has an inner diameter equal to 287 mm, and it is approximately 7 m long with a piston (a loudspeaker with flat membrane) in one end and a carefully designed termination in the other end, providing a standing wave ratio that is very close to 24 dB between 100 Hz and 700 Hz. With 287 mm inner diameter the cut-on frequency for the first non-plane-wave mode is almost exactly at 700 Hz. The array is too big to be mounted in a cross-section of the tube, but by mounting the array with the array plane parallel with the tube axis, a condition is obtained where there is ideally zero intensity normal to the array plane, and where there is ideally equal pressure on the two parallel array planes. At 700 Hz, the length of the array is approximately equal to half a wavelength, so in the frequency range up to 700 Hz the array will cover less than half a wavelength. With a standing wave ratio near 24 dB the sound field consists of a dominating standing wave part and a much smaller propagating component. So if the array is centred at a pressure maximum, then there will be a dominating pressure distribution that has no phase variation and a slow amplitude variation across the array. A good estimate of the p-RI index could therefore be

8

obtained by use of equation (2). This would, however, require the pressure and intensity data to be available over the full mapping area for use in the equation. Because this could not be easily done, a p-RI index based on readings of the peak levels from the pressure and intensity maps was chosen:

$$R_{peak} \equiv 10 \cdot \log\left(\frac{\left| p_{measured} \right|^2 {}_{max}}{\left| I \right|_{max}} \right) \tag{3}$$

Here the pressure maximum is taken over the front array layer and the intensity maximum is taken over the calculation area.

All data to be presented were taken with the array in the position shown in Fig. 4. One of the array microphones was used as a reference, and 100 averages were taken with an FFT analyser with 800 Hz bandwidth and 400 frequency lines. The resulting record length was sufficient to ensure good coherence between the reference and all array positions.

Fig. 4. Pictures of the DLA in the standing wave tube
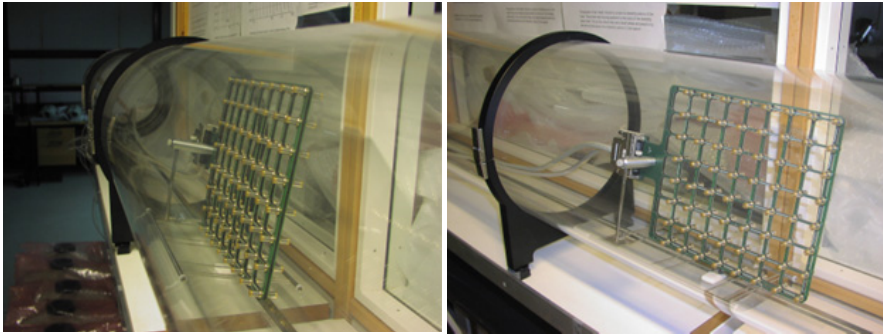
Fig. 5 shows the sound pressure distribution on the front microphone layer of the array at two frequencies – (left) low and (right) high – where the array is centred at a pressure maximum in the standing wave pattern. The region of maximum pressure is the most demanding for intensity estimation, because a small active propagating component has to be extracted in the presence of a much stronger standing wave component. Fig. 6 shows the corresponding vector intensity maps on the front array plane, estimated using SONAH after application of TEDS-based correction for differing microphone frequency responses. The

constant energy flow density of the small propagating part of the sound field is fairly well identified although its pressure is approximately 12 dB weaker than the standing wave component. A few microphones could be better compensated though. The vector intensity map estimated without use of TEDS-based correction is shown in Fig. 7. Clearly, at the low frequencies the p-I index of the sound field is too high to allow an estimation of the intensity vectors without microphone response correction.

Fig. 5. Sound pressure on the front array layer at (left) low (measured pressure at 212 Hz) and (right) high frequency (measured pressure at 674 Hz)
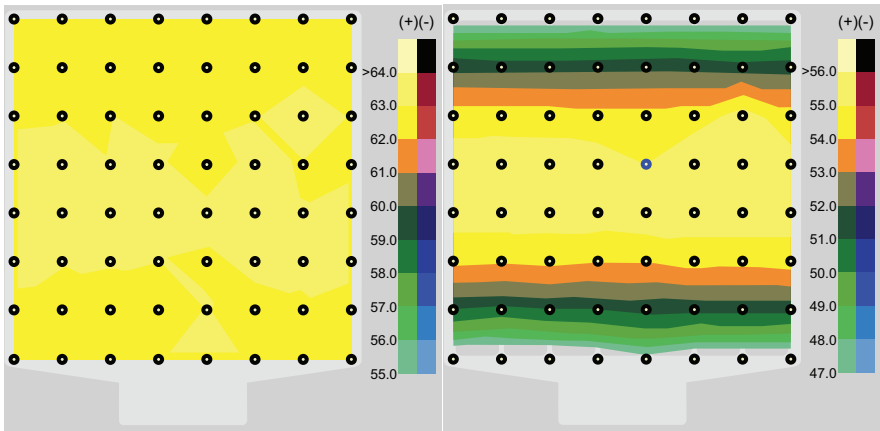
Fig. 6. In-plane vector intensity calculated after TEDS correction: Left at 212 Hz
and right at 674 Hz
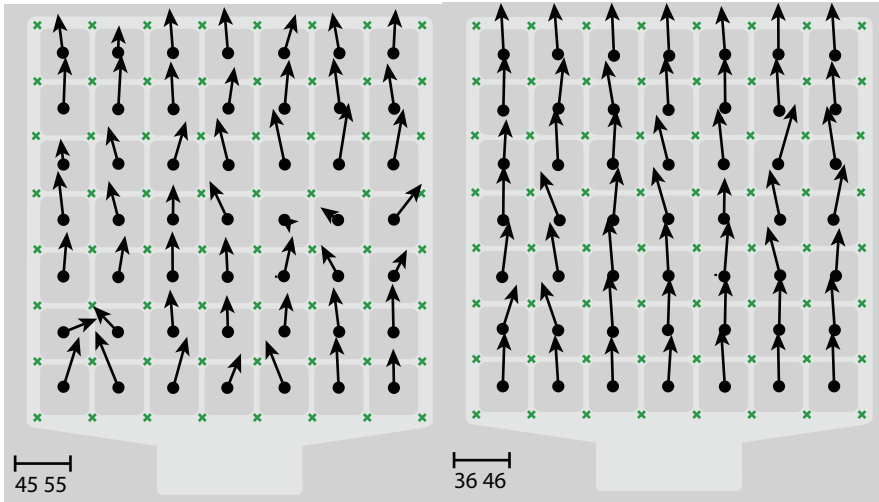
Fig. 7. In-plane vector intensity calculated without TEDS correction: Left at 212 Hz
and right at 674 Hz
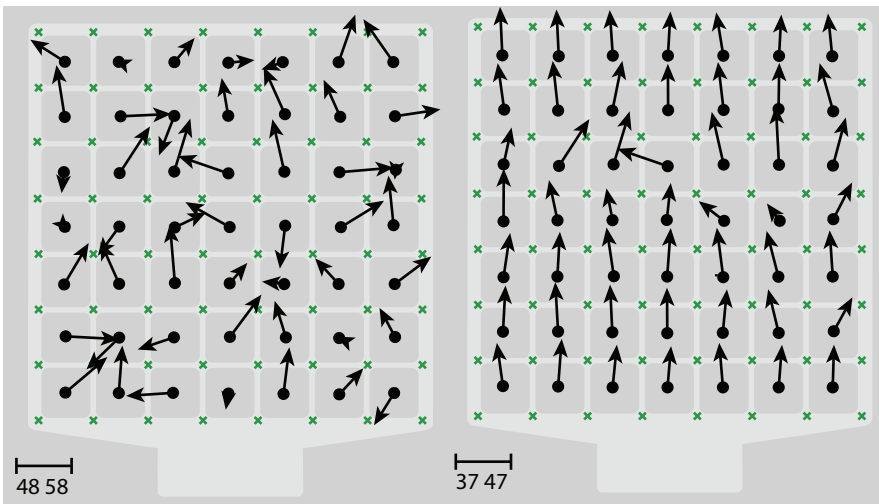
Typically the estimation of the sound intensity component normal to the array surface is more useful than estimation of the in-plane vector component. In the present set up, the normal component is very close to zero, because the array is aligned to be parallel with the tube axis. As explained previously we can then estimate the p-RI index at frequencies, where the array is centred at a maximum of the standing wave pattern. The frequencies represented in Fig. 5 to Fig. 7 are such frequencies. Fig. 8 shows the estimated normal intensity 15 mm in front of the DLA ($z = -15$mm) for those frequencies when TEDS correction has been applied, and Fig. 9 shows the corresponding maps without TEDS correction..

Fig. 8. Normal intensity 15 mm in front of the array using TEDS correction: Left at 212 Hz and right at 674 Hz
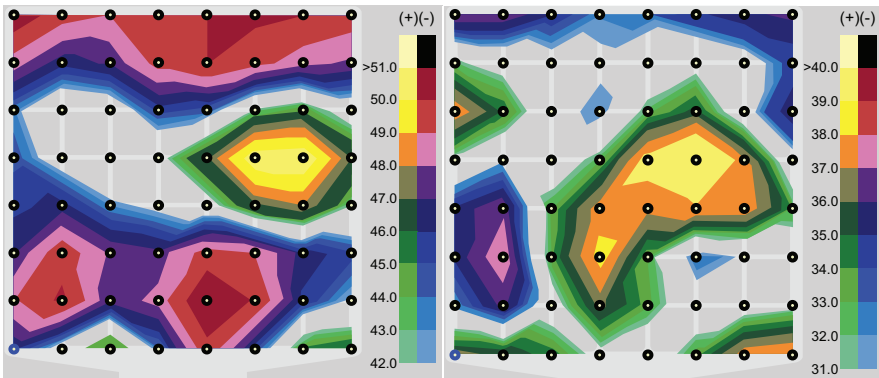
Fig. 9. Normal intensity 15 mm in front of the array without TEDS correction: Left at 212 Hz and right at 674 Hz

Peak level readings from Fig. 5(left) and Fig. 8(left) lead to a 212 Hz estimate of the p-RI index around 13 dB, when TEDS is applied. Similar readings from Fig. 5(left) and Fig. 9(left) lead to an index around 6 dB when TEDS is not applied. More precise peak level readings at a larger set of frequencies, where the array is centred at a pressure maximum, leads to the p-RI index spectra shown in Fig. 10. This figure also shows the corresponding simulated p-RI index spectra from Fig. 3 for comparison

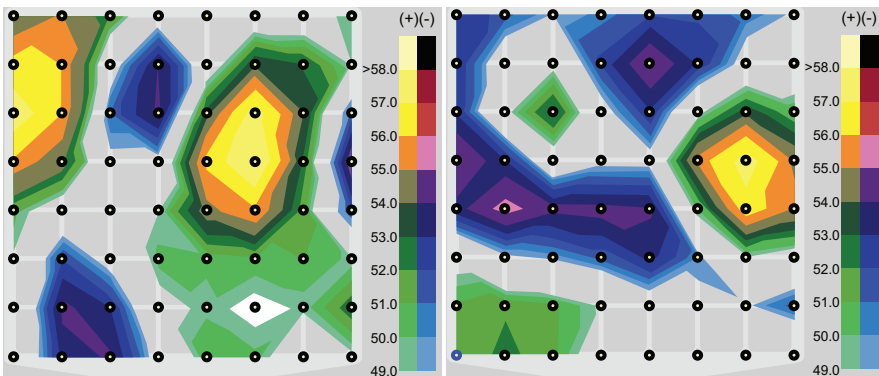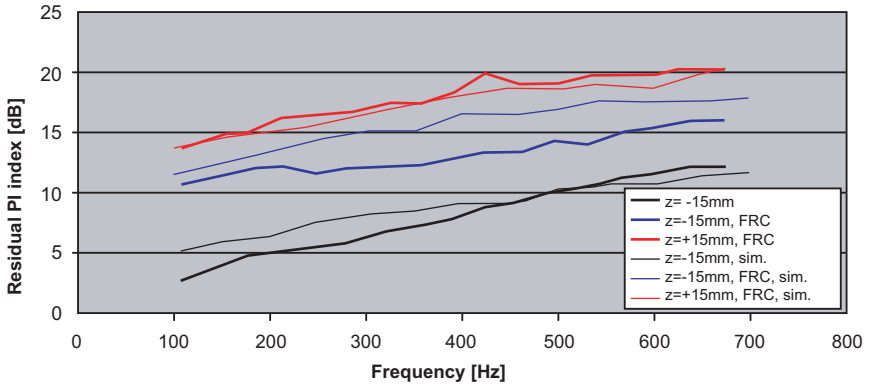*Fig. 10. Measured residual p-RI index spectra for intensity normal to array plane*

The general trend (see Fig. 10) is for measured and simulated p-RI index spectra to agree quite well. On the array centre plane (red curves), there is very good agreement, showing that the simulated phase error distribution over the interval $\pm 0.4°$ is a good model when TEDS correction is applied. On the centre plane, the SONAH calculation is very accurate, so the residual intensity is probably due to phase errors. For the calculation 15 mm in front of the array ($z = -15$ mm), SONAH calculation errors will contribute much more to the residual intensity, and the SONAH reconstruction will tend to amplify the phase errors, explaining why the residual intensities increase and the index spectra therefore decrease. The decrease is seen to be stronger for the measured index spectrum than for the simulated spectrum. The explanation is probably that for the case of the measured data, other errors, such as diffraction in the array grid, will also be amplified by the SONAH reconstruction and therefore contribute much more to the residual intensity at $z = -15$ mm than on the centre plane, $z = +15$ mm. Finally, we look at the black curves in Fig. 10, representing measured and simulated p-RI index spectra 15 mm in front of the DLA when TEDS correction is not applied. A likely explanation for the

different slopes of the two spectra is that the typical microphone phase mismatch is not constant over the considered frequency band, and tends to be largest at the lowest frequencies. At the high frequency end, the phase mismatch interval of $\pm 2°$ (assumed in the simulations) is probably too wide. Use of a narrower interval in the simulations would lift up the simulated index spectrum in the high frequency end, causing the simulated spectrum to be consistently above the measured one, which should be expected because the measured spectrum will have contributions from other sources of error than the phase mismatch as explained above.

The rather good agreement between measurement and simulation (with explainable differences) gives confidence that the measured p-RI index spectra in Fig. 10 constitute a good measure of the dynamic capability of DLA/SONAH in extracting a small active intensity component in the presence of a strong reactive field component.

Measurements in Under-pressure Chamber

A special problem in connection with in-flight measurements is the significant drop in static pressure, even in a pressurized cabin. Apart from the influence on air density and propagation speed of sound, the static pressure drop will also affect the microphone frequency responses, and to some extent these changes will differ from microphone to microphone, in particular at the low frequencies. This is because the low frequency cut-off is defined by the mass and stiffness of the diaphragm system, and some of the stiffness is due to the air cavity behind the diaphragm. This cavity will differ slightly in volume from microphone to microphone.

To investigate, to which extent the level of static pressure drop experienced during typical flight conditions will cause the microphone responses to diverge, we took the DLA to the Danish Aviation Medicine Centre, which has a depressurization chamber. This chamber can reproduce the static pressure variations occurring during typical flights. Table 1 shows the static Pressure variation, the temperature and the simulated altitude as functions of time during the simulated flight that the DLA was exposed to.

In order to measure, how the microphone frequency responses changed relative to each other during the simulated flight, the DLA was put in an acoustic cavity excited in such a way that microphones in a single layer would be exposed to nearly identical pressures up to approximately 200 Hz. Fig. 11 shows a picture of the box cavity, which has six speakers coupled in parallel and mounted in the top plate. By putting the DLA horizontally in the box, all microphones in a horizontal

layer will experience very accurately the same pressure at frequencies well below the first box resonance. The pressure difference between the two layers is very small, but we shall consider here only microphones in a single layer..

Table 1. Simulated flight description

Altitude	Pressure		Temperature	Accumulated Time
Feet	mm Hg	hPa	°C	minute.second
Sea Level		1022		0
4000	656.40	875.13	20.5	7.00 – 17.10
6000	609.09	812.05	20.7	20.40 – 30.20
8000	564.58	752.71	2	34.40 – 45.25
Sea Level		1021		54.00

Fig. 11. Pictures of acoustic cavity for measuring relative microphone responses: Left is a closed calibration box and right is open
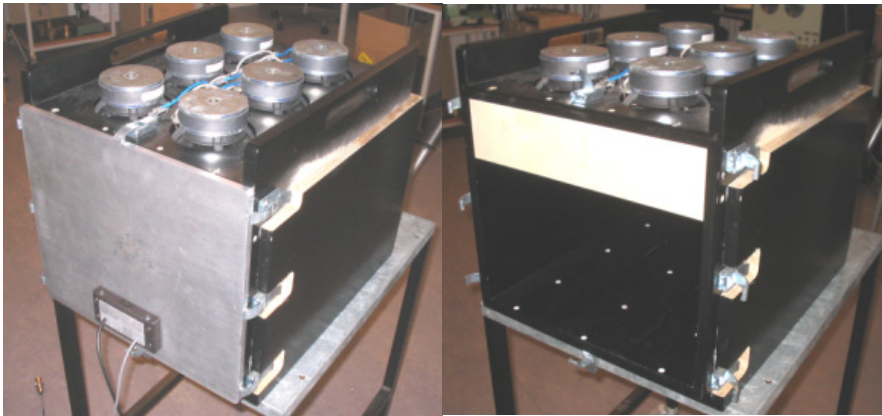
Beyond the DLA, a reference microphone with very low sensitivity to static pressure changes was put in the cavity. At each level during the simulated flight (sea level; 4000, 6000 and 8000 ft; and sea level), responses of all microphones relative to the reference were measured. By subtracting the initial 'sea level' responses from all subsequently measured responses for the individual microphones, response changes of all 64 microphones in a layer could be monitored.

15

Fig. 12 shows, how the phase responses changed at 4000 ft. The ripples in the range 200 – 250 Hz are due to some first vibrations in the otherwise very stiff walls of the cavity – not to acoustic resonances. When these ripples are disregarded, the typical low frequency spreading due to differing low-frequency cut-off frequencies is clearly observed, and the phase deviations seem to decay with increasing frequency as would be expected. Above 200 Hz it seems that the phase spreading does not exceed ±0.25º (relative to an average of the microphone responses).

Fig. 12. Phase changes of 64 microphones at 4000 ft
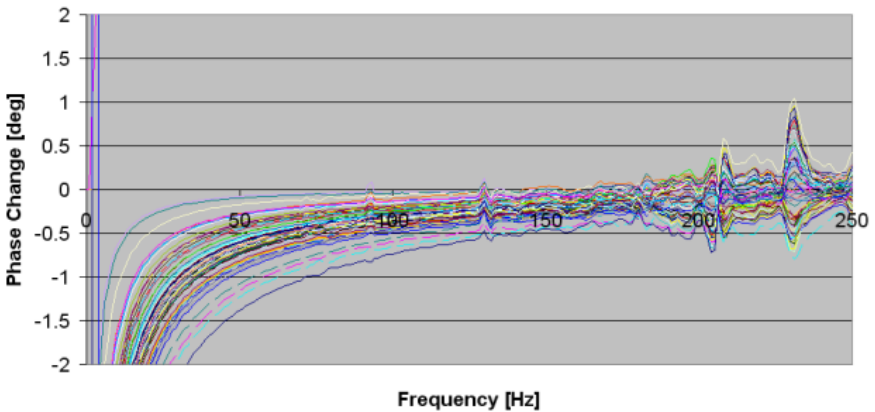
Fig. 13. Phase changes of 64 microphones at 8000 ft

16
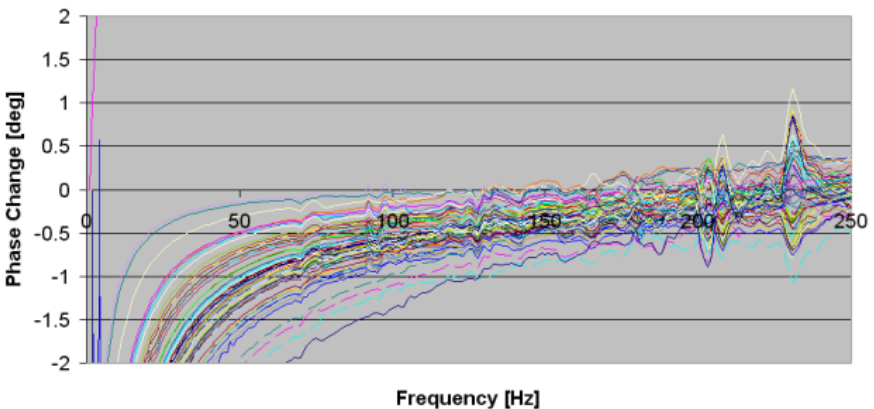
Fig. 13 contains corresponding phase change curves measured at 8000 ft simulated altitude. The general changes follow the same trend, only now the phase spreading has been approximately doubled, so above 200 Hz the spreading seems to stay within ±0.5º. In a pressurized cabin the static pressure is normally not allowed to drop below the pressure at 8000 ft, so Fig. 13 represents in that sense the worst case scenario.

Back at sea level the microphone responses should return to the reference responses measured just before the simulated flight. Fig. 14 confirms that this happens. The small deviations that can be observed are mainly due to a small temperature change, the influence from wall vibrations and measurement uncertainties.

Fig. 14. Phase changes of 64 microphones back at sea level

After - Phase changes
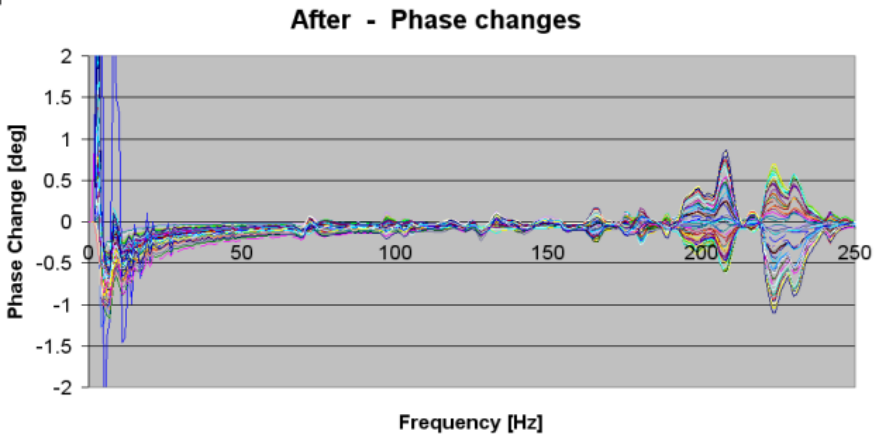
Conclusions

The **Simulated Measurements** and **Measurement in Standing Wave Tube** sections presented simulated and real measurement with the DLA/SONAH system to clarify the performance of the system at low frequencies, in particular its ability to measure a small active intensity component in the presence of a strong reactive or diffuse-field component. This ability was quantified through spectra of Pressure-Residual Intensity index. The investigation showed that TEDS-based

correction of microphone frequency responses provided an essential improvement of the dynamic capability of the system.

Combining the observations from the depressurization measurements with the results from **Simulated Measurements** and **Measurement in Standing Wave Tube** on the sensitivity of the DLA/SONAH to transducer mismatch leads to the following conclusions:

1) Below approximately 200 Hz an in-flight response-calibration of the individual microphones would be required to achieve an acceptable dynamic range.

2) Above approximately 200 Hz an acceptable dynamic range can be achieved by just applying the TEDS based correction.

References

[1]   A. Röder, A. Peiffer, et. al.: "Definition of the Acoustic Environment in Typical Aircraft and Helicopter Cabin." CREDO deliverable DWP1.1 (2006)

[2]   Various authors: "Definition of the Aircraft Industry Requirements." CREDO deliverable 1.2 (2006)

[3]   J. Hald: "Patch Near-field Acoustical Holography Using a New Statistically Optimal Method", *Proceedings of InterNoise 2003* (2003)

[4]   J. Hald: "Patch holography in cabin environments using a two-layer handheld array with an extended SONAH algorithm." *Proceedings of Euronoise 2006* (2006)

[5]   J. Gomes: "Comparing Parameter Choice Methods for the Regularization in the SONAH Algorithm." *Proceedings of Euronoise 2006* (2006)

[6]   J. Hald, J. Morkholt, et. al.: "Array based measurement of radiated and absorbed sound intensity components." *Proceedings of Acoustics 8 (Euronoise)* (2007).

[7]   M. Bach-Andersen: "Computer Simulations of diffraction effects in the double layer array at high frequencies." CREDO deliverable DWP2.2 (2007)

Calculating the Sound Field in an Acoustic Intensity Probe Calibrator – A Practical Utilisation of Boundary Element Modelling[*]

Erling Sandermann Olsen, Vicente Cutanda,
Johan Gramtorp and Anders Eriksen

Abstract

The newest generation of sound intensity measurement equipment is small and light enough to be hand-held when used for measurements in the field. This increases the need for field verification of the equipment. Field verification must be easy to perform and should not require the equipment to be taken apart. Therefore, it was decided at Brüel & Kjær to develop an intensity probe calibrator that could be used for the two-microphone intensity probe as it is, without dismounting the spacer. The geometry of the cavity of the calibrator with probe is rather complex, and it turned out that a simple model based on geometric considerations could not be made for predicting the acoustic properties of the calibrator. Therefore, a boundary element model of the calibrator cavity was developed and successfully used in the design of the calibrator. The calculations are briefly described, and the sound fields in the coupler with different cavity geometries and source configurations and the corresponding microphone responses are discussed.

Résumé

Les nouveaux équipements dédiés aux mesurages d'intensité acoustique sont suffisamment compacts et légers pour être tenus à la main dans le cadre d'opérations sur le terrain. Mais cela pose aussi des exigences en terme de vérification de leur calibrage. Celle-ci doit être facile à réaliser et ne doit pas nécessiter le démontage de l'instrumentation. C'est pourquoi Brüel & Kjær a décidé de mettre au point un calibreur de sonde acoustique utilisable avec la sonde d'intensimétrie à deux microphones sans avoir à démonter le bloc d'espacement.

---

[*] First published in Proceedings of the Eighth International Congress on Sound and Vibration, 2001

La forme de la cavité du calibreur avec sonde étant relativement complexe, il était impossible de prévoir les propriétés acoustiques du calibreur au moyen d'un modèle exclusivement basé sur des considérations géométriques. Un modèle à éléments finis de frontière de la cavité du calibreur a donc été développé et utilisé avec succès dans la conception du calibreur. Les calculs sont ici décrits succintement, et la discussion porte sur les champs acoustiques générés dans le coupleur avec des formes de cavité et configurations de source différentes, et sur les réponses correspondantes des microphones.

Zusammenfassung

Die Schallintensitätsmesssysteme der neuesten Generation sind so klein und leicht, dass die Geräte bei Messungen vor Ort in der Hand gehalten werden können. Aus diesem Grund besteht ein größerer Bedarf an Vor-Ort-Überprüfungen der Messausrüstung. Überprüfungen vor Ort müssen unkompliziert und möglichst ohne Auseinandernehmen der Ausrüstung auszuführen sein. Deshalb beschloss Brüel & Kjær, für die Intensitätssonde mit zwei Mikrofonen einen Kalibrator zu entwickeln, der angewendet werden kann, ohne das Distanzstück zu entfernen. Die Geometrie des Hohlraums des Kalibrators mit Sonde ist recht komplex und es stellte sich heraus, dass ein einfaches Modell auf der Basis geometrischer Überlegungen zur Vorhersage der akustischen Eigenschaften des Kalibrators nicht geeignet war. Deshalb wurde ein Randelementmodell des Kalibratorhohlraums entwickelt und bei der Konstruktion des Kalibrators mit Erfolg angewendet. Die Berechnungen werden kurz beschrieben und die Schallfelder im Kuppler mit verschiedenen Hohlraumgeometrien und Schallquellenkonfigurationen und den entsprechenden Mikrofonfrequenzgängen diskutiert.

Introduction

The newest generation of sound intensity measurement equipment is small and light enough to be hand-held when used for measurements in the field. The hand-held Brüel & Kjær Sound Intensity System Type 2270-G is a good example of such measurement equipment. As in all measurements, the equipment for sound intensity measurements must be calibrated and verified before and after use. While in the laboratory it is not so important how the calibration is made, field calibration and verification must be easy to perform and should not require the equipment to be taken apart. Since this is not the case with sound intensity

calibrators available until now, it was decided at Brüel & Kjær to develop a new intensity probe calibrator for field use. The design goals for the calibrator were:

- That it could be used for the Brüel & Kjær ½" two-microphone intensity probe as it is, without dismounting the spacer
- That it should be usable for absolute sensitivity calibrations as well as for pressure residual intensity index verification
- That it should fulfil the requirements of International Standards IEC 60942 Type 1 and IEC 61043 Class 1

A prototype for the new calibrator was designed based on classical, sound acoustical considerations (for example, symmetry and as small a volume as feasible around the probe). The design of the prototype was not far from the design of the final Brüel & Kjær Sound Intensity Calibrator Type 4297, but it turned out to work in a much smaller frequency band than expected. The unexpected behaviour was discussed intensively, and the prototype underwent a number of modifications. The behaviour could not be explained by means of any suggested geometrical, lumped parameter or impedance considerations, and no significant improvements were achieved with the modifications. Therefore, it was decided to make a numerical model in order to find an explanation of the sound field behaviour in the coupler and to see if there were any possibilities of improvement. Since one of the authors, Vicente Cutanda, was working with Boundary Element Modeling (BEM) of microphone interiors at the same time, a model of the coupler could quickly be implemented with his software.

Geometry

The calibrator consists of an axisymmetrical coupler cavity where the complete probe with spacer can be inserted. Basically, the coupler is a cylindrical cavity in which the intensity probe is placed with mutual symmetry axis and symmetry plane. In the prototype the coupler cavity was connected to another cavity with the sound source and a reference microphone through a small hole in the wall midway between the microphone diaphragms. In the final design the sound source is a part of a ring source situated in the coupler wall midway between the microphones and connected to the cavity through a slit (Fig. 1).

The cavity in the final design is also connected to another cavity with a reference microphone, but that is of minor importance in this context. The geometry of the coupler cavity is illustrated in Fig. 1 and the calibrator with the coupler is shown in its final design in Fig. 2.

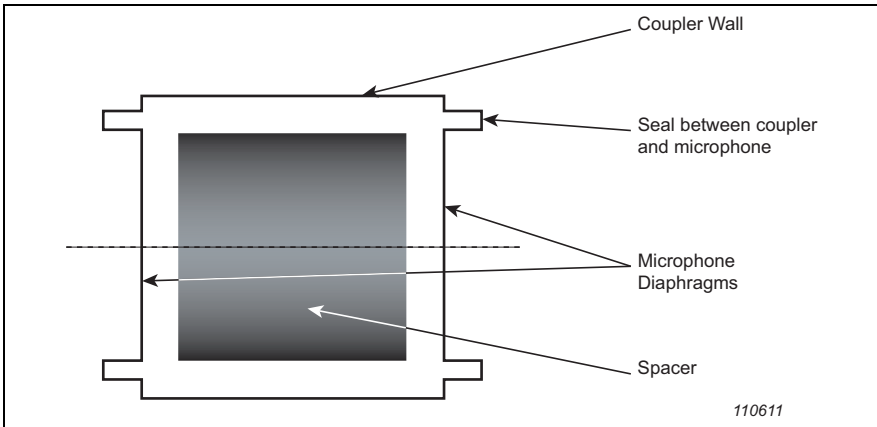*Fig. 1. Coupler geometry defined for the calculations*

Fig. 2. The final calibrator. The probe is a ½" probe with a 12 mm spacer. The slit with the sound source is seen in the middle of the coupler cavity


22

Calculations

The BEM method used for the calculations was the direct collocation method in a formulation for axisymmetric bodies [1] with an improved calculation method for near-singular integration [2]. The actual formulation used allows for the calculation of non-axisymmetric sound fields by using a cosine expansion of the acoustical variables, i.e., pressure, particle velocity and excitation [3]. The terms in the expansion represent a sound field with an increasing number of nodelines. The first term, $m = 0$, represents the axisymmetric part of the sound field and the following terms represent the non-axisymmetric part of the sound field. In this case, a non-axisymmetric velocity distribution on the boundary was used for the excitation. No losses were taken into consideration in the calculations, and the microphone diaphragms were assumed to be blocked.

Calculations were made for a wide variety of dimensions and shapes within the basic geometry of the coupler cavity. Here a few of the calculations are presented to demonstrate the influence of the variations and the important results. In the examples, the sound source is a half-ring source in the coupler wall at the symmetry plane of the probe spacer (in the middle of the coupler). Also, one of the microphones is slightly displaced from its correct position so that the gaps between the spacer and the diaphragm are different at the two microphones.

The condition number of the coefficient matrix is a convenient means to locate the eigenfrequencies of the coupler [4]. This is due to the instability generated in the system of equations in the vicinity of such eigenmodes. Since the condition number is a measure of the system ill-conditioning, it presents maxima at those frequencies. In Fig. 3 the condition numbers are shown for the system of equations for the first four terms of the cosine expansion. Whereas the eigenfrequencies of the configurations with the spacer do not correspond in a simple way to the dimensions of the coupler, the eigenfrequencies for the configuration without the spacer correspond closely to what must be expected for a cylindrical cavity. With the spacer, the frequency of the axisymmetric modes increases with increasing diameter while the frequency of the non-axisymmetric modes decreases with increasing diameter.

The calculated sound fields in the coupler at frequencies close to the eigenfrequencies shown in Fig. 3 are shown for the modes below 10 kHz in Fig. 4 through Fig. 7. In the narrow coupler the lowest eigenmode is an axisymmetric longitudinal mode. Note that the phase is opposite at the two microphone diaphragms. This will not be the case if the gaps at the microphones are exactly same. However, the sound field is unstable at this frequency and will change

Fig. 3. Coupler with different diameter and with and without spacer. Half-ring source. Condition number plots for the first four terms in the cosine expansion of the sound field: a) 14.4 mm with spacer; b) 16.0 mm with spacer; c) 17.0 mm with spacer; d) 16.0 mm without spacer
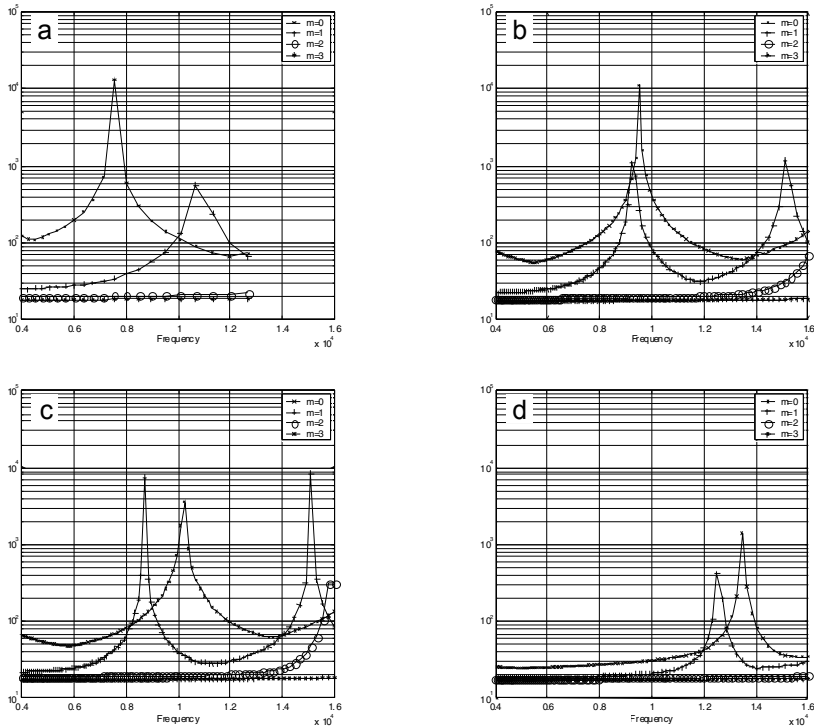
with any small change in the dimensions. The lowest modes of the 16.0 mm and 17.0 mm coupler are transversal modes. The sound field is in opposite phase in the two sides of the coupler and the sound pressure level is high. The 16.0 mm coupler has a longitudinal mode at a slightly higher frequency. The sound field at that frequency is a combination of a transversal and longitudinal wave..

Fig. 4. Sound field at 7.55 kHz in ∅ 14.4 mm coupler with spacer and half-ring source. a) modulus in dB; b) phase in °

110613
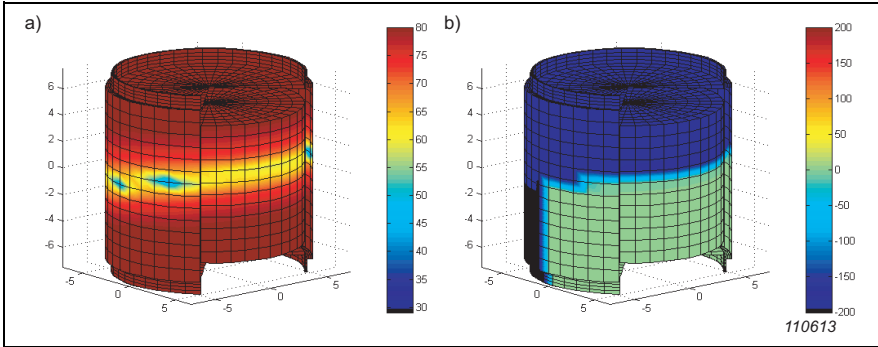
Fig. 5. Sound field at 9.38 kHz in ∅ 16.0 mm coupler with spacer and half-ring source: a) modulus in dB; b) phase in °

110614
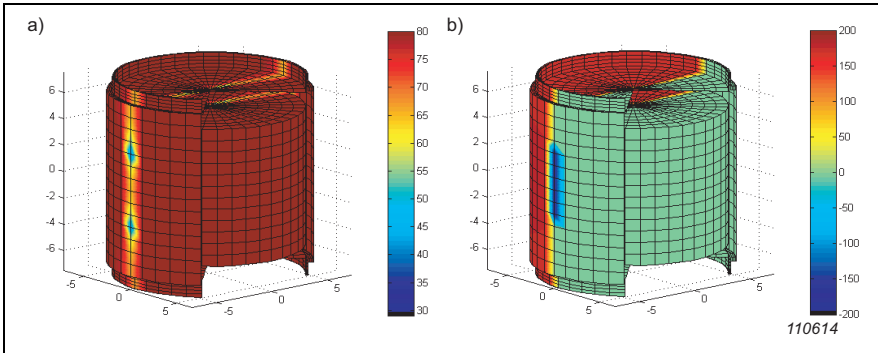
Discussion

As shown above, the sound field in the coupler with the same excitation changes rapidly with the coupler diameter in a way so that there is an optimal diameter for the coupler cavity with the given geometry. With a small diameter and thus a narrow gap between the probe and the coupler walls the axisymmetric modes appear at lower frequencies than the non-axisymmetric modes. With increasing diameter the frequencies of the axisymmetric modes increase while the frequencies for the non-axisymmetric modes decrease. The optimum diameter is

Fig. 6. Sound field at 9.51 kHz in ⌀ 16.0 mm coupler with spacer and half-ring source: a) modulus in dB; b) phase in °
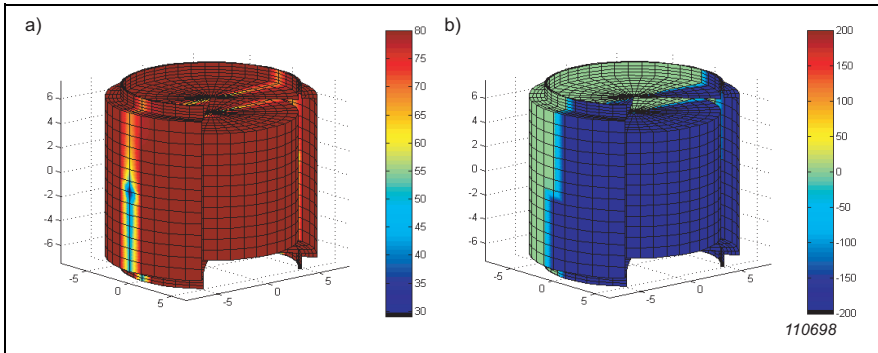
Fig. 7. Sound field at 8.72 kHz in ⌀ 17.0 mm coupler with spacer and half-ring source: a) modulus in dB; b) phase in °
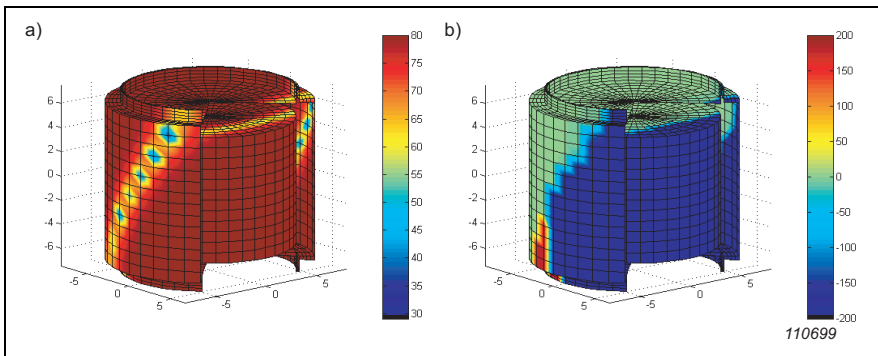
the diameter where the modes have the same frequency since this gives the highest bandwidth without resonances and thereby a stable sound field.

The changes of the sound field with diameter illustrates why the modes of the cavity with the spacer cannot be found with simple geometrical considerations. The cavity cannot be divided into substructures that can be identified as being cavities, tubes or transmission lines. Rather, all parts of the cavity with the spacer are something in between such acoustical elements.

The process in the development project on which this paper is based clearly shows the value of numerical calculation methods. The advantage most often mentioned in the literature is the possibility of making many virtual prototypes,

26

that is, testing many variants of a design. However, a more important advantage of using the calculations here is that a deeper understanding of the sound field in the coupler and the problems in the development were obtained.

Based on the calculations described in the previous section the coupler in the intensity probe calibrator was designed with a diameter of 16.0 mm. In the first design of the coupler the diameter was chosen to be as small as practically possible. It was actually discovered before the calculations were taken into use that some, but not all, couplers with a larger diameter had a better performance, but since there were no clear explanations and since it is not practically possible to make several prototypes this did not lead to a conclusion on the design. Furthermore, even more prototypes may not have led to the final design since the information on the sound field and thereby the explanation of the differences could only have been obtained with highly complicated measurements on many prototypes.

The microphone responses were also considered during the development of the coupler. In principle the microphones are only sensitive to the axisymmetrical modes of the sound field and therefore non-axisymmetric modes should not influence the performance. Although any real microphone may exhibit some minor sensitivity to non-axisymmetrical modes this is probably not the only reason the coupler does not perform well when non-axisymmetric modes are present. Rather, because the sound field varies so much in the coupler near the eigenfrequencies, the axisymmetric part of the sound pressure in the real coupler may very well be a little different at the two microphones, and this difference would be measured even with perfect microphones. For this reason it is not possible to compare directly the calculations with measurements with the probe in the coupler and therefore such comparisons are not shown here. What could be seen was that the couplers performed well at frequencies up to around 2/3 of an octave below the first eigenfrequency of the coupler. It should be remembered that in this context good performance means less than 0.1 dB and 0.2° difference between the two microphones at frequencies around 5 kHz.

The Sound Intensity Calibrator Type 4297 that is the result of the development project described here is very close to the fulfillment of the design goals initially set up for the project. Without the spacer the calibrator fulfils the requirements of IEC 61043 Class 1. The pressure-residual intensity index of the sound field is larger than 24 dB in 1/3-octave bands from 50 Hz to 6.3 kHz. However, with the spacer the pressure-residual intensity index is slightly lower than 24 dB in the 6.3 kHz 1/3-octave band. The calibrator can still be used for verification of the

equipment with the spacer in daily use, but it does not fulfill the standard completely. The numerical calculations showed that this was the best performance that could be achieved for a coupler where the probe could be inserted without dismounting the spacer.

Conclusions

In this paper it has been demonstrated how BEM calculations successfully led to a working design of a sound intensity calibrator. The sound field in the coupler could not be predicted with 'classical' methods. The calculations did not only lead to a successful design but also gave an understanding of the behaviour of the sound field in the calibrator that could not be obtained without the calculations.

The calculations described in this paper led a development project from failure into success. Numerical calculations are certain to be developed and used in future acoustical design projects at Brüel & Kjær.

Acknowledgements

The authors wish to thank Peter Møller Juhl at Odense University in Denmark for his contributions to the work with the calculations described here. The authors also wish to thank Erling Frederiksen at Brüel & Kjær and Finn Jacobsen at the Technical University of Denmark for valuable discussions during the development of the intensity calibrator.

References

[1]   A.F. Seybert, B. Soenarko, F.J. Rizzo, D.J. Shippy: "A Special Integral Equation Formulation for Acoustic Radiation and Scattering for Axisymmetric Bodies and Boundary Conditions." *J. Acoust. Soc. Am.*: 80, 1241 – 1247 (1986)

[2]   V. Cutanda, P.M. Juhl, F. Jacobsen: "On the Modeling of Narrow Gaps using the Standard Boundary Element Method." *J.Acoust. Soc. Am.*: 109, 1296 –1303 (2001)

[3]   P.M. Juhl: "An Axisymmetric Integral Equation Formulation for Free Space Non Axisymmetric Radiation and Scattering of a Known Incident Wave." *J. Sound Vib.*: 163, 397 – 406 (1993)

[4]   M.R. Bai: "Study of Acoustic Resonance in Enclosures using Eigenanalysis Based on Boundary Element Methods." *J. Acoust. Soc. Am.*: 91, 2529 – 2538 (1992)

Multi-field Microphone – When the Sound Field is Unknown[*]

Svend Gade and Niels V. Bøgholm

Abstract

Only a small percentage of all acoustical measurements are performed in the well-defined and well-controlled environment of a calibration laboratory – most acoustical measurements are done under non-controlled conditions that in many cases are not even known beforehand. This is why some acoustical standards such as the IEC 61672 series (the "Sound Level Meter standard") specify the performance of the measuring microphone over a wide range of environmental conditions.

Modern quality measuring condenser microphones often meet or exceed the requirements even under very varying conditions. However one important – and unfortunately in many cases major – source of error is often neglected: the response of the actual microphone type in the actual sound field. The influence of different sound fields on the measurement error is discussed in some detail with practical examples and it is shown how a worst-case error exceeding 10 dB @ 20 kHz is a real risk.

After a brief discussion of condenser microphone design rules, it is shown how the use of new technology has made it possible to develop a new condenser microphone that drastically reduces the error caused by the influence of an unknown sound field or varying angle of incidence. Finally, test results from production samples of the new microphone are shown.

Résumé

Le pourcentage de mesurages acoustiques réalisés dans les conditions d'essai draconiennes du type centre d'étalonnage est très faible. La plupart du temps, les mesures acoustiques sont obtenues dans des conditions environnementales non

---

contrôlées, voire même non connues à l'avance. C'est pourquoi certaines normes acoustiques comme la série CEI 61672 (la norme " Sonomètres ") spécifient les performances du microphone de mesure sous différentes conditions environnementales.

Or, si les microphones à condensateur actuels satisfont aux critères exigés, voire les dépassent, même dans des conditions d'essai très fluctuantes, une cause d'erreur, souvent grave malheureusement, a tendance à être négligée : la réponse du type de microphone utilisé dans le champ acoustique mesuré. L'influence de différents champs acoustiques sur l'erreur de mesurage est ici discutée de manière détaillée au moyen d'exemples concrets, et il est montré que, dans le pire des cas, une erreur de plus de 10 dB à 20 Hz est un risque réellement encouru.

Après de brèves considérations sur les règles qui président à la conception des microphones à condensateur, il est montré comment une nouvelle technologie a permis le développement d'un nouveau microphone à condensateur qui réduit de manière drastique l'erreur associée aux champs acoustiques de type non connu ou aux angles d'incidence fluctuants. L'article se termine par une présentation des résultats d'essai de divers spécimens du nouveau microphone, fabriqués en usine.

Zusammenfassung

Nur ein Bruchteil aller akustischen Messungen wird unter den wohldefinierten und kontrollierten Bedingungen eines Kalibrierlaboratoriums ausgeführt – im Gegenteil, die meisten akustischen Messungen erfolgen unter nicht kontrollierten Bedingungen, die in vielen Fällen nicht einmal vorher bekannt sind. Deshalb wird in mehreren akustischen Standards wie der Normenreihe IEC 61672 (die "Schallpegelmesser-Norm") die Leistung des Messmikrofons über einen weiten Bereich von Umgebungsbedingungen angegeben.

Moderne hochwertige Kondensator-Messmikrofone erfüllen oder übertreffen häufig die Anforderungen, auch bei sehr wechselnden Bedingungen. Eine wichtige - und in vielen Fällen leider bedeutungsvolle – Fehlerquelle bleibt jedoch häufig unberücksichtigt: das Verhalten des aktuell verwendeten Mikrofontyps im vorliegenden Schallfeld. Der Einfluss verschiedener Schallfelder auf den Messfehler wird anhand von praktischen Beispielen ausführlich erörtert und es

wird gezeigt, dass im ungünstigsten Fall Fehler von mehr als 10 dB bei 20 kHz möglich sind.

Nach einer kurz gefassten Erläuterung der Konstruktionsregeln für Kondensatormikrofone wird gezeigt, wie mit Hilfe neuer Technologie ein neues Kondensatormikrofon entwickelt werden konnte, das den durch unbekannte Schallfelder oder unterschiedliche Einfallswinkel verursachten Fehler drastisch reduziert. Schließlich werden Testergebnisse gezeigt, die mit Produktionsmustern des neuen Mikrofons erhalten wurden.

Introduction

Only a small percentage of all acoustical measurements are performed in a well-defined and well-controlled (for example, defined as: Temperature 23°C, Relative Humidity 50% and Ambient Static Pressure 101.3 kPa) environment of a calibration laboratory – in fact, most acoustical measurements are done under non-controlled conditions that are not even known beforehand.

This is the reason that acoustical standards such as the IEC 61672 series (the "Sound Level Meter standard") specify the performance of the measuring microphone over a wide range of environmental conditions. When using high-quality instrumentation and transducers, the varying environmental conditions normally cause no problems at all.

However, one major source of error remains – the impact that the nature of the sound field will have on the measurement uncertainty. It is common practice to assume that the sound field in any measurement will be a free, diffuse or pressure field.

Sound Fields

- Free field: There are no reflecting objects, only the microphone disturbs the sound field

- Diffuse field: There are so many reflecting surfaces that the sound waves arrive with equal probability from all directions

- Pressure field: This is found in small confined spaces like calibration couplers

Depending on the nature of the sound field, an appropriate microphone is selected: a microphone which is "optimised" for the sound field in question. Unfortunately, there are many practical situations where the sound field is not really of a well-defined type. This may be the case inside buildings, during in-cabin noise measurements or measurements on multiple or non-stationary sources. Often a free-field microphone is chosen, based more on tradition than on real knowledge about the nature of the actual sound field. Fig. 1 shows a picture of the Multi-field Microphone, which can be used in any of the above-mentioned sound fields.

Fig. 1. Multi-field Microphone Type 4961

080204/2

It is amazing how large the potential errors are if the conditions are non-ideal. Fig. 2 shows the response of a free-field microphone in a true free field; the frequency response is the ideal flat response. But the angle of incidence may not be zero (as assumed in Fig. 2) or the sound field may not be a true free field; say it was actually diffuse instead of free and the response would be as shown in Fig. 3.
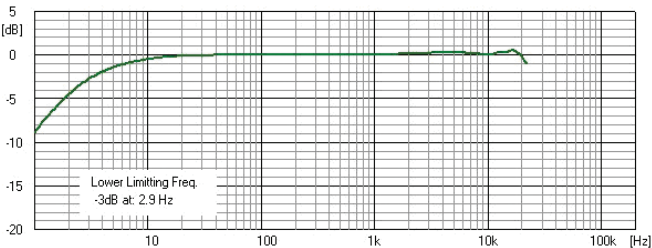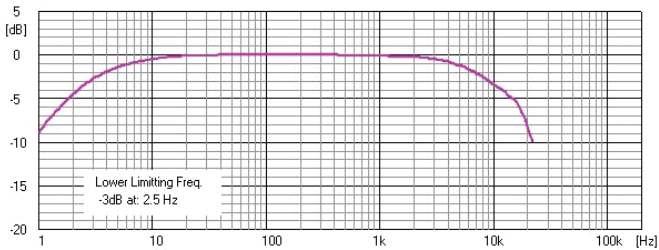
Fig. 2. Free-field response of a ½" free-field microphone

*Fig. 3. Diffuse-field response of a ½″ free-field microphone*

Both Fig. 2 and Fig. 3 are valid for a typical ½″ microphone with protection grid and (in Fig. 2) for zero degrees angle of incidence (i.e., the microphone diaphragm is facing head-on towards the sound source).

Actually, taking not only the nature of the sound field but also the angle of incidence into consideration, the potential error may be even larger.

Fig. 4 shows the maximal error as a function of frequency when a free-field (Type 4189/90), and a diffuse-field (Type 4942) microphone are being used in a field or at an angle of incidence for which the microphone was not optimised.

Fig. 4. Maximal error
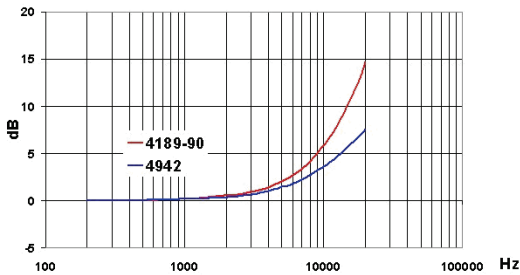
As is clearly shown in Fig. 4, the error is noticeable from 2 kHz and already at around 6 kHz the potential maximal error due to "unknown conditions" largely exceeds the influence of all other environmental factors and even exceeds the IEC 61672 tolerance of 3.5 dB, not to mention the IEC 61094 ± 2 dB requirement.

Is there a Cure?

It has been known for many years [1, 3, 4] that a microphone disturbs the sound field and that the issues addressed here are caused solely by the physical size of the microphone.

Generally speaking a microphone can be considered non-diffractive as long as $(\pi/\lambda)2a \leq 1$, where λ is the wavelength and $2a$ the microphone diameter. Therefore, a ½″ microphone can measure without disturbance of the sound field up to 10 kHz, whereas a ¼″ microphone can measure up to 20 kHz. In reality, microphones can measure up to higher frequencies, because the measurement error at higher frequencies is predictable and the microphone frequency response can be compensated for (optimised) in the microphone itself. In this way, a flat frequency response can be achieved – but only in one given kind of sound field.

That is why there exist three different microphone types: Free-field, diffuse-field and pressure-field microphones. As mentioned above, a ¼″ microphone would be readily usable in all fields up to 20 kHz, but today, unfortunately, all commercial ¼″ measuring microphones have less sensitivity and much higher noise floor than their ½″ counterparts. A typical ¼″ free-field microphone has a noise floor around 40 dB(A) as opposed to 16 – 18 dB(A) for a typical premium quality ½″ free-field microphone.

The Limiting Factors

In order to discuss the most important factors that determine the sensitivity of a condenser microphone, we will introduce a set of simple equations that describe the sensitivity of a condenser microphone.

The microphone mid-range pressure sensitivity M_p (V/Pa) can be expressed as the product of two sensitivities $M_p = M_e M_m$.
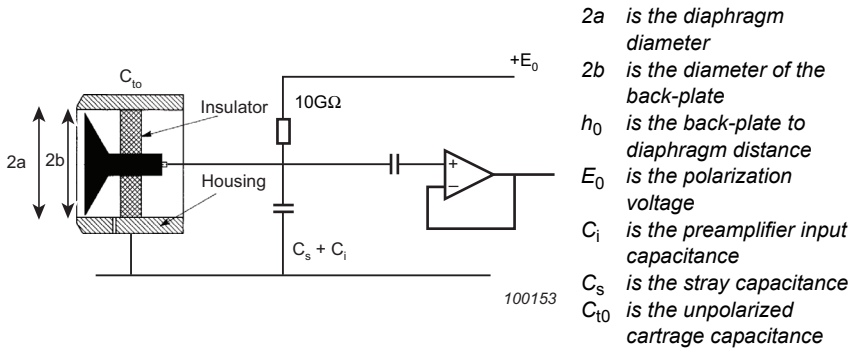
Here M_e is the electrical transfer function in V/m, M_m is the mechanical transfer function in m/Pa and, as one observes, the dimension of M_p is [V/m] [m/Pa], which means that M_p is in V/Pa as expected.

As shown in the literature (for example, [2]) the following equations apply:

$$M_e = E_0/h_0 \, [1 - b^2/2a^2] \, [1 + (C_i + C_s)/C_{t0}]^{-1} \tag{1}$$

In most practical cases b (see Fig. 5) equals approximately 0.8 a and typically $C_i + C_s \ll C_{t0}$; hence, (1) is, with good approximation:

Fig. 5. Principle schematic of a condenser microphone with preamplifier

2a is the diaphragm diameter
2b is the diameter of the back-plate
h_0 is the back-plate to diaphragm distance
E_0 is the polarization voltage
C_i is the preamplifier input capacitance
C_s is the stray capacitance
C_{t0} is the unpolarized cartrage capacitance

$$M_e = [0.68\,E_0]/h_0 \tag{2}$$

For the mechanical transfer function in m/Pa, [2] shows that:

$$M_m = a^2/8T \tag{3}$$

where T is the tension of the diaphragm in N/m, which depends on the radial stress s_{rr} (N/m^2) and the thickness d of the diaphragm according to:

$$T = s_{rr}\,d \tag{4}$$

In practical cases, T is often in the interval 2000 – 3000 Pa.
Combining equations (2) and (3), the simplified equation for the microphone mid-range sensitivity is:

$$M_p = M_m\,M_e = [k\,E_0\,a^2] / [T\,h_0] \tag{5}$$

Typical values for a normal ¼" cartridge are:

- Polarization voltage E_0 200 V
- Backplate diameter 2b = 4 mm
- Tension T 2000 – 3000 Pa
- k is a constant

Suggestions on How to Increase the Sensitivity of a ¼″ Microphone

By inspection of equation (5), it is very easy to see how to increase the sensitivity of a microphone:

- Increase the polarization voltage
- Decrease the distance between the back-plate and the diaphragm
- Reduce the diaphragm tension

Short Comments and Limitations to the Suggestions

Increased Polarization voltage: For externally polarized microphones the polarization voltage must be 200 V in order to be compatible with existing front-ends on the market.

Besides there are practical limitations determined by the arcing and static diaphragm deflection and for these and other reasons the polarization voltage cannot be changed.

Reduction of the back-plate to diaphragm distance is also dangerous since this increases the electrical field strength with increased risk of sparks (excess noise in the microphone).

The last resort is to have a much lower diaphragm tension but here there are severe limitations when using stainless steel as the diaphragm material.

Instead, a solution has been found using a titanium diaphragm; this diaphragm has the benefit that if it is processed properly the tension can be reduced to such a low value that the sensitivity of the ¼″ microphone is very close to that of a normal ½″ high-sensitivity microphone.

The low tension means that the resonance frequency for this microphone is much lower than for a normal ¼″ microphone – around 26 kHz instead of say 70 to 100 kHz.

Additional sensitivity increase has been achieved by using more of the outer diameter (of the 6.25 mm) for the active part of the microphone, i.e., a larger *b* value than in a normal ¼″ microphone.

In order to achieve excellent temperature stability, the cartridge was made "all titanium", which brings additional benefits with respect to corrosion resistance and insensitivity to magnetic fields,.

A new titanium housed ¼″ Constant Current Line Drive (DeltaTron) preamplifier with TEDS (Transducer Electronic Data Sheet) has been developed

in order to be able to offer a complete all-titanium microphone with multi-field performance, see Fig. 1.

In summary, the microphone described here has the following key parameters:

Diameter	¼″
Sensitivity	60 mV/Pa
Noise floor	< 20.5 dB(A)
Frequency range	5 Hz – 20 kHz
Dynamic range	20 – 130 dB
Upper SPL limit	130 dB (3% distortion)
Max SPL	> 150 dB (peak)
Temperature	–20 to +80°C (–4 to +176°F)

Fig. 6 shows the performance in an unknown field for a multi-field microphone compared with the already mentioned ½″ microphones used today. Fig. 7 shows a typical calibration chart for a multi-field microphone.

*Fig. 6. Multi-field FRF compared against IEC 61672 limits and ½″ microphones*
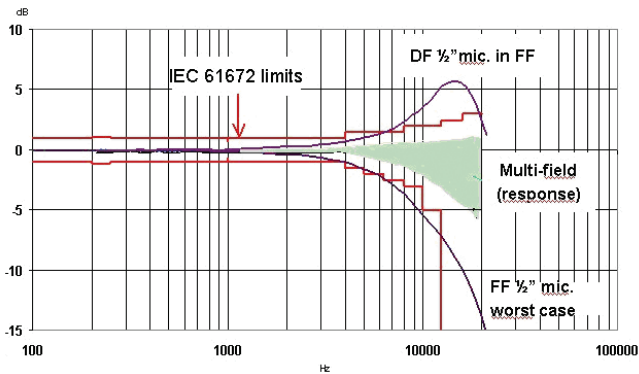
Conclusions

Using all-titanium techniques combined with new unique techniques, it has been possible to overcome the limitations that traditional technologies and materials have so far imposed on ¼″ microphones. The result is a microphone that widely eliminates the influence of unknown measurement conditions and additionally releases the user from the pain of being forced to choose between different microphones. Its main uses are measurement in unpredictable sound-field

Fig. 7. Multi-field Frequency responses: Free-field response (upper), Diffuse-field response (middle) and minimum response (lower)
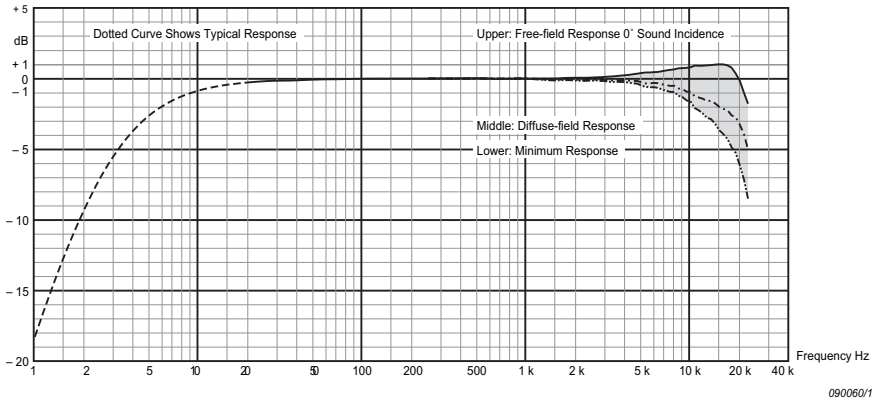
conditions, cabin noise measurements, near-field measurements and ad hoc sound measurements.

The multi-field measuring microphone, Type 4961, is the only ¼″ true measuring microphone in the world with a typically 20 dB noise floor and sensitivity exceeding 50 mV/Pa – enabling it to make accurate measurements in free, diffuse or diverse sound fields. Because Type 4961 is small and relatively insensitive to the angle of incidence, it simplifies the process of making complex sound measurements, saving technicians' valuable time planning, setting up and analyzing results.

References

[1] "Free Field Response of Condenser Microphones." *Brüel & Kjær Technical Review*:1 and 2 (1959)

[2] *AIP Handbook of Condenser Microphones*; Eds. G.S. Wong and T.E.W. Embleton, American Institute of Physics, New York: p. 43

[3] *Theory; Microphone Handbook Vol. 1 (BE 1447-11)*; Brüel & Kjær Sound & Vibration Measurements A/S (1996)

[4] *Falcon Range Microphones; Microphone Handbook Vol. 2 (BE 1373-12)*; Brüel & Kjær Sound & Vibration Measurements A/S (1995)

Previously issued numbers of
Brüel & Kjær Technical Review

(Continued from cover page 2)

1 – 1998   Danish Primary Laboratory of Acoustics (DPLA) as Part of the National
Metrology Organisation
Pressure Reciprocity Calibration – Instrumentation, Results and Uncertainty
MP.EXE, a Calculation Program for Pressure Reciprocity Calibration of
Microphones
1 – 1997   A New Design Principle for Triaxial Piezoelectric Accelerometers
A Simple QC Test for Knock Sensors
Torsional Operational Deflection Shapes (TODS) Measurements
2 – 1996   Non-stationary Signal Analysis using Wavelet Transform, Short-time
Fourier Transform and Wigner-Ville Distribution
1 – 1996   Calibration Uncertainties & Distortion of Microphones.
Wide Band Intensity Probe. Accelerometer Mounted Resonance Test
2 – 1995   Order Tracking Analysis
1 – 1995   Use of Spatial Transformation of Sound Fields (STSF) Techniques in the
Automative Industry
2 – 1994   The use of Impulse Response Function for Modal Parameter Estimation
Complex Modulus and Damping Measurements using Resonant and Non-
resonant Methods (Damping Part II)
1 – 1994   Digital Filter Techniques vs. FFT Techniques for Damping Measurements
(Damping Part I)
2 – 1990   Optical Filters and their Use with the Type 1302 & Type 1306 Photoacoustic
Gas Monitors
1 – 1990   The Brüel & Kjær Photoacoustic Transducer System and its Physical
Properties
2 – 1989   STSF – Practical Instrumentation and Application
Digital Filter Analysis: Real-time and Non Real-time Performance

Special technical literature

Brüel & Kjær publishes a variety of technical literature that can be obtained from your
local Brüel & Kjær representative.

The following literature is presently available:

• Catalogues
• Product Data Sheets

Furthermore, back copies of the Technical Review can be supplied as listed above.
Older issues may be obtained provided they are still in stock.

www.bksv.com